How to estimate aortic characteristic impedance from magnetic resonance and applanation tonometry data?

E. Bollache, N. Kachenoura, I. Bargiotas, A. Giron, A. de Cesare, M. Bensalah, D Lucor, A. Redheuil, E. Mousseaux

How to estimate aortic characteristic impedance from magnetic resonance and applanation tonometry data?

Short title: Best estimate of aortic impedance in CMR

Emilie BOLLACHE[a,b,c,d], PhD, Nadjia KACHENOURA[a,b,c], PhD, Ioannis BARGIOTAS[a,b,c], MS, Alain GIRON[a,b,c], PhD, Alain DE CESARE[a,b,c], PhD, Mourad BENSALAH[a,b,c], MD, Didier LUCOR[d], PhD, Alban REDHEUIL[a,b,c,e], MD, PhD, Elie MOUSSEAUX[f,g], MD, PhD

[a]Sorbonne Universités, UPMC Univ Paris 06, UMR 7371, UMR_S 1146, Laboratoire d'Imagerie Biomédicale, 75013 Paris, France

[b]INSERM, UMR_S 1146, Laboratoire d'Imagerie Biomédicale, 75013 Paris, France

[c]CNRS, UMR 7371, Laboratoire d'Imagerie Biomédicale, 75013 Paris, France

[d]UMR CNRS 7190 / UPMC, Institut Jean le Rond d'Alembert, 75005 Paris, France

[e]Institut de Cardiologie, Hôpital Pitié Salpêtrière, 75013 Paris, France

[f]Cardiovascular Imaging, Medical Imaging Department, Hôpital Européen Georges Pompidou, APHP, 75015 Paris, France

[g]INSERM, UMR 970, PARCC, 75015 Paris, France

Conflicts of interest: None declared.

Correspondence and requests for reprints:

Emilie Bollache

Laboratoire d'Imagerie Biomédicale (LIB) - UMR_S 1146 Inserm / UPMC

CHU Pitié-Salpêtrière

91 boulevard de l'Hôpital

F-75634 Paris Cedex 13, France

Fax number: +33 1 53 82 84 48

Telephone number: +33 1 53 82 84 37

Email address: emilie.bollache@imed.jussieu.fr

Word count: 6402 words

Number of tables: 2

Number of figures: 4

Number of supplementary digital content files: 0

Abstract

Objectives. Compare seven previous methods for the estimation of aortic characteristic impedance, which contributes to left ventricle (LV) pulsatile load, from phase-contrast cardiovascular magnetic resonance (PC-CMR) and applanation tonometry data. **Methods.** We studied 77 healthy (43±16years) and 16 hypertensive (61±9years) subjects, who consecutively underwent ascending aorta CMR and carotid tonometry resulting in flow and pressure waveforms, respectively. Characteristic impedance was semi-automatically estimated in time domain from these latter waveforms, using 7 methods. Methods were based on: 1-4: magnitudes at specific times; 5: early-systolic up-slope; 6: time-derivatives peak; and 7: pressure-flow loop early-systolic slope. **Results.** Aortic characteristic impedance was significantly increased in hypertensive patients when compared to elderly controls (n=32) with a similar mean age (59±8years) when using methods based on 95% of peak flow, up-slopes and derivatives peaks ($p<0.05$). When considering healthy subjects, impedance indices were significantly correlated to central pulse pressure for all methods ($p<0.005$). Finally, characteristic impedance was correlated to the frequency domain reference values ($r>0.65$, $p<0.0001$), with a slight superiority for the same three methods as above ($r>0.82$, $p<0.0001$). **Conclusions.** This is the first study demonstrating PC-CMR and tonometry usefulness in aortic characteristic impedance temporal estimation. Methods based on 95% of peak flow as well as those based on derivatives peaks and up-slopes, which are fast and independent of curves pre-processing, were slightly superior. They can be easily integrated in a clinical workflow and may help to understand complementarity of this pulsatile index with other CMR aortic geometry and stiffness measures in the setting of LV-aortic coupling.

Condensed abstract

This is the first study reporting aortic characteristic impedance temporal estimation from CMR flow and applanation tonometry pressure. Such index, contributing to left ventricle (LV) pulsatile load, was semi-automatically estimated in the ascending aorta, while comparing in 93 normotensive and hypertensive subjects seven previously reported methods. Methods based on 95% of peak flow, pressure-to-flow derivatives peaks and up-slopes ratio were slightly superior in distinguishing hypertensive patients from mean age-matched controls, and in terms of association with reference frequency domain impedance. Such fast and straightforward methods can be easily integrated in clinical workflow and prove as clinically useful in LV-aortic coupling.

Keywords: aortic characteristic impedance; velocity-encoded magnetic resonance; applanation tonometry; pulsatile load

Introduction

Structural and hemodynamic alterations of large conduit arteries, occurring with aging[1-3] as well as other aggravating factors and leading to arterial stiffness[4], have been associated with increased cardiac and cerebral mortality[2, 3]. Proximal aortic characteristic impedance (Zc_{Ao}), defined as the pressure change generated by a given flow wave change in the absence of reflections[5], is an index related to both local stiffness and geometry. It contributes to the pulsatile arterial load faced by left ventricle (LV) during ejection and has been shown to be an independent predictor of LV mass index[6]. Most studies, using invasive[7-18] and non-invasive[9, 19-21] techniques, estimated Zc_{Ao} in humans in the frequency domain as the aortic input impedance averaged over high frequencies to minimize the effects of reflected waves. Other studies used simpler and faster time domain methods to calculate Zc_{Ao}, based on the early systolic part of pressure and flow waveforms, where reflections effects are supposedly negligible. Such studies used either invasive data from animals[22-24] and humans[12], or applanation tonometry of the carotid artery combined with Doppler echocardiography of the LV outflow tract (LVOT)[6, 20, 21, 25-29], and showed good agreement between temporal estimates and the reference frequency domain values[12, 20-22].

Cardiovascular magnetic resonance (CMR) is already used in clinical routine for reference LV systolic and global function evaluation and several studies also demonstrated its usefulness in the non-invasive estimation of aortic stiffness indices[4, 30-33]. Although phase-contrast (PC)-CMR sequences enable an accurate measurement of blood flow velocities with high temporal resolutions[34, 35], to our knowledge, only one study used CMR data to calculate Zc_{Ao} in the time domain[36],

but from aortic areas estimated from steady-state free-precession (SSFP) sequences, rather than aortic flows.

Accordingly, our aims were 1) to non-invasively estimate ascending aorta characteristic impedance in the time domain in healthy normotensive and hypertensive subjects using a semi-automated analysis of aortic PC-CMR flow and carotid applanation tonometry pressure curves, based on 7 methods previously reported in the literature, 2) to test which methods are able to characterize hypertensive patients as compared against controls with a similar mean age, and 3) to investigate which methods are better associated with the reference frequency domain characteristic impedance, as well as with carotid pulse pressure.

Methods

Study population

We studied 77 healthy subjects free from overt cardiovascular disease (31 women; mean age: 43±16 years [19-79 years]) and 16 patients with hypertension (as defined by either systolic blood pressure ≥ 140 mmHg, diastolic blood pressure ≥ 90 mmHg, or current treatment for hypertension; 5 women, mean age: 61±9 years [50-81 years]). The study protocol was approved by the institutional review board, and all participants were informed and provided signed consent in accordance with the declaration of Helsinki.

Data acquisition

Cardiovascular magnetic resonance

Each subject underwent CMR imaging of the thoracic aorta using a 1.5 Tesla GE system (Signa, General Electric Medical Systems, Waukesha, Wisconsin, USA) with cardiac phased array coil (eight channels).

First, axial cine images were acquired, during breath-holding, using a fast retrospectively gated gradient echo SSFP sequence, in the mid-ascending aorta perpendicular to the aorta at the level of the center of the right pulmonary artery (Figure 1.A), using the following typical scan parameters: repetition time (TR) = 3.4 ms, echo time (TE) = 1.4 ms, flip angle = 50°, views per segment = 6, slice thickness = 6 mm, pixel spacing = 0.76x0.76 mm^2, matrix = 224x192 and temporal resolution = 10 ms after applying a view sharing technique.

Then, the same slice location was used to acquire PC images, using a 2D through-plane velocity-encoded sequence with retrospective gating during breath-holding (Figure 1.B and C). Averaged acquisition parameters were: TR = 7.4 ms, TE = 3.0 ms, flip angle = 20°, number of excitation = 1, views per segment = 2, slice thickness = 8 mm, pixel spacing = 1.64x1.64 mm^2, acquisition matrix = 256x128, encoding velocity = 200 cm/s. To minimize background offsets and so that acquisition duration remained compatible with breath-holding, a 50% rectangular field of view was used. View sharing was also used, resulting in an effective temporal resolution of 15 ms. The imaged structure was always at the centre of the acquired image to minimize PE-wraparound effects.

Blood pressures

First, an oscillometric sensor cuff was used to assess blood pressure at the brachial artery (Vital Signs Monitor, Welch Allyn Inc, USA) in the magnet simultaneously to aortic CMR acquisitions. Three measurements were averaged.

Then, applanation tonometry of right carotid artery was performed using the Pulse Pen device (Diatecne, Milano, Italy)[37] immediately after CMR acquisitions. At least two acquisitions of over 10 consecutive waveforms were performed with a temporal resolution of 2 ms. Pressures were calculated after rescaling tonometric measurements by brachial mean and diastolic pressures measured during CMR acquisitions[1], to account for potential arterial condition changes between CMR and tonometric examinations. Carotid pressure waveforms were averaged for each subject over several cardiac cycles while visually excluding irregular cardiac cycles, which presented a mismatch between pressures at the beginning and the end of the cycle. On average, 7 [3-12] cardiac cycles were taken into account to calculate carotid pressure waveforms. Carotid pulse pressure (cPP) was calculated as the difference between carotid systolic and diastolic blood pressures.

Data analysis and characteristic impedance estimation

Contours of the ascending aorta (AA) were automatically detected for all phases of the cardiac cycle on both SSFP and PC modulus images (Figure 1.B) using the validated ArtFun software (U.678 Inserm / UPMC)[38], which has been previously used in various studies on large populations[4, 33, 39]. Such segmentation resulted in AA lumen area variations from SSFP data and AA flow curves from PC data, after superimposition of modulus contours on velocity images (Figure 1.C).

Estimation of local aortic pulse wave velocity

Local AA pulse wave velocity was calculated from AA distensibility as $PWV_{AO} = 1 / \sqrt{(\rho \cdot \text{AA distensibility})}$, according to the Bramwell-Hill model[30, 40], where $\rho = 1059\ kg.m^{-3}$ is blood density and AA distensibility is calculated as $(As - Ad) / (Ad \cdot cPP)$, As and Ad being respectively systolic and diastolic AA lumen areas.

Estimation of aortic characteristic impedance

A custom software, developed and integrated to an interface in Matlab (Mathworks, Natick, MA, USA), was used to superimpose tonometry carotid pressure and PC-CMR AA flow waveforms that were oversampled with a 1 ms temporal step. Then, to account for the distance between carotid and aortic measurement locations, early systolic up-slopes of the pressure and flow waveforms were interpolated using linear regressions, and feet of the two resulting lines were shifted to the beginning of the cardiac cycle[6, 21, 22]. In addition, to take into account potential changes in heart rate between CMR and tonometric acquisitions that would induce different systolic and diastolic durations, the systolic and diastolic phases of the two waveforms were individually temporally interpolated to the mean duration value. Prior to this interpolation, systolic and diastolic phases were manually defined by the dicrotic notch for pressure curves and the first zero crossing for flow curves. Finally, automated peak and minima detection, area under curve and time derivatives calculation (Figure 2.A-C) were integrated to the software, to estimate characteristic impedance, using 7 previously described methods:

1) $Zc_{AoQmax} = (P_{Qmax} - cDBP) / Q_{max}$[12], where cDBP is carotid diastolic blood pressure, Q_{max} is peak flow and P_{Qmax} is pressure magnitude at peak flow (Figure 2.A);

2) $Zc_{AoQ95\%max} = (P_{Q95\%max} - cDBP) / (Q_{95\%max} - Q_{min})$[20] where $Q_{95\%max}$ and Q_{min} are flow at 95% of its peak value and at its minimal value, respectively, and $P_{Q95\%max}$ is pressure magnitude at 95% of peak flow (Figure 2.A);

3) $Zc_{AoPi} = (P_i - cDBP) / Q_{max}$[5], where P_i is pressure at inflection point corresponding to the initial upstroke of the reflected pressure wave (Figure 2.A);

4) $Zc_{AoSV} = ES \cdot (P_i - cDBP) / 2 \cdot SV$[41], where ES is systolic duration and SV is stroke volume (Figure 2.A);

5) $Zc_{Aoslopes} = P_{slope} / Q_{slope}$[12], where P_{slope} and Q_{slope} are pressure and flow early systolic up-slopes, respectively (Figure 2.A);

6) $Zc_{Aoderiv} = P'_{max} / Q'_{max}$[12] where P'_{max} and Q'_{max} are peaks of pressure and flow time derivatives, respectively (Figure 2.B).

7) Zc_{loop} was derived from pressure-flow loop as the slope of the linear interpolation of its early systolic part (Figure 2.C)[12].

Of note, original pressure and flow curves, before temporal shift and resizing, were used for methods 5 and 6.

Pressure and flow curves were also used to estimate in the frequency domain aortic input impedance magnitude, calculated for each harmonic as the ratio between fast Fourier transform moduli of pressure and flow (Figure 2.D). Reference aortic characteristic impedance (Zc_{AoF}) was then calculated by averaging input impedance between the frequency of its first local minimal value and 15 Hz[42], while excluding noisy magnitudes that are out of the range defined by input impedance mean magnitude ± 2 times its standard deviation, over this frequency range.

Statistical analysis

Mean values and standard deviations (SD) were provided for continuous variables. For comparison of baseline characteristics, central blood pressures, aortic diameter, pulse wave velocity and characteristic impedance between “young” (below 50 years) and “elderly” healthy subjects (above 50 years), as well as between the hypertensive patients and the elderly normotensive subjects with a similar mean age, a nonparametric Mann–Whitney test was used. For comparisons on the whole group of healthy subjects of time domain characteristic impedance against their reference frequency counterpart as well as carotid pulse pressure, linear regression was used. For all comparisons, Pearson correlation coefficients were provided. Further significance of the difference between such dependent correlations was also evaluated using an Hotelling-Steiger test[43]. Briefly, given three variables X_1, X_2 and X_3 and r_{ij} the correlation coefficient obtained for comparison between X_i and X_j, the Hotelling-Steiger test is $t = (r_{12} - r_{13}) \sqrt{\frac{(n-1)(1+r_{23})}{2\frac{n-1}{n-3}|R| + \frac{(r_{12}+r_{13})^2}{4}(1-r_{23})^3}}$, where n is sample size and $|R| = 1 - r_{12}^{\ 2} - r_{13}^{\ 2} - r_{23}^{\ 2} + 2r_{12}r_{13}r_{23}$. Such test, while testing whether $\rho_{12} = \rho_{13}$, follows a Student's *t*-distribution with *n*-3 degrees of freedom. In our case, X_1 is frequency Zc_{AoF} or carotid pulse pressure, while X_2 and X_3 are temporal Zc_{Ao} estimated using two methods we want to compare. In addition, degree of agreement between time domain methods and the frequency domain reference was assessed by Bland-Altman analysis and mean biases as well as limits of agreement, defined as [mean bias-1.96xSD; mean bias+1.96xSD], were reported. All reported p-values are two-sided and a p-value of less than 0.05 indicated statistical significance. Statistical

analysis was achieved using Stata 10 IC (StataCorp LP, College Station, Texas, USA).

Results

Baseline characteristics, central blood pressures as well as aortic diameter, pulse wave velocity and characteristic impedance estimated in the frequency and time domains are summarized in Table 1 for young and elderly healthy subjects as well as hypertensive patients. By design, there was no significant difference in age between elderly healthy subjects and patients with hypertension. Also, gender distribution was the same in the three groups. All subjects had a body mass index BMI <30 kg/m², except for two hypertensive patients who had BMI of 30.7 kg/m² (70 year-old male) and 31.1 kg/m² (72 year-old male). Central blood pressures were within normal range for healthy subjects, and systolic, diastolic as well as mean blood pressures were significantly higher for elderly subjects when compared to young subjects. Furthermore, as expected, both ascending aortic diastolic diameter and pulse wave velocity were increased in old subjects. An increasing trend was observed in hypertensive patients as compared to the elderly group for aortic pulse wave velocity and blood pressures, but did not reach statistical significance except for pulse pressure. Finally, while aortic characteristic impedance was not different between young and elderly healthy subjects whichever temporal or frequency methods are used, it was significantly increased in hypertensive patients when compared to the elderly subjects, when using the reference frequency domain method as well as temporal methods based on 95% of peak flow and up-slopes and time derivatives peaks ratios. Such changes in characteristic impedance are illustrated on the aortic input impedance spectra averaged over the groups of young healthy subjects, elderly

healthy subjects and elderly hypertensive subjects provided in Figure 3. When studying gender-related differences in aortic characteristic impedance, all frequency and time domain methods resulted in no change in young healthy subjects, while in the elderly healthy subjects higher values were observed in women compared to men. Figure 4 illustrates such gender-differences in characteristic impedance when estimated using the reference frequency method as well as the temporal method based on 95% of flow peak, which is the most commonly reported time domain method. Over the 77 healthy subjects, all temporal aortic characteristic impedance estimates were significantly correlated to central pulse pressure, with a correlation coefficient slightly superior for the method based on up-slopes ratio (Table 2). However, this superiority was not significant. For comparisons of the 7 temporal Zc_{Ao} against Zc_{AoF} reference values estimated in the frequency domain, Pearson correlation coefficients as well as Bland-Altman mean biases and limits of agreement are provided in Table 2. All relationships were significant with again a slight overall superiority in terms of correlation coefficient when using the method based on up-slopes. While association between the up-slopes method and the frequency domain reference was superior than associations obtained for methods 1, 3, 4 and 7 (Zc_{AoQmax}: $p=0.0002$; Zc_{AoPi}: $p=0.0001$; Zc_{AoSV}: $p<0.0001$; Zc_{Aoloop}: $p=0.002$, respectively), they were equivalent to those of methods based on 95% of peak flow and time derivatives peaks ratio. Finally, Bland-Altman analysis indicated an overall underestimation of time domain methods when compared to the frequency domain reference and this underestimation was lower in terms of mean bias for the time derivatives peaks ratio method.

Discussion

Characteristic impedance of the proximal aorta is defined as the ratio between pressure wave change and the corresponding flow change, in the absence of reflections[5]. Thus, it contributes to the pulsatile component of LV afterload, and was shown to be an independent predictor of LV mass index[6]. The majority of previous studies estimated human Zc_{Ao} in the frequency domain[7-21], which is considered to be the reference method. Other studies estimated human Zc_{Ao} in the time domain using early systolic parts of pressure and flow waveforms, before reflections arrival, from either invasive pressure and flow data[12] or applanation tonometry carotid pressure combined with LVOT flow measured using Doppler echocardiography[6, 20, 21, 25-29]. However, in the majority of Doppler echocardiography-based studies, flow was calculated as LVOT maximal velocities multiplied by LVOT[20, 21, 26, 27, 29] or aortic[25, 28] area, measured on a single phase of the cardiac cycle, and used as a surrogate for aortic flow. Besides, LVOT area was estimated from diameter while neglecting its non-circular shape[44]. In addition, Doppler studies using LVOT flow instead of aortic flow to assess aortic impedance assume that such flows are comparable during early systole, despite the differences in geometry and elastic properties between the two locations. Indeed, such similarity in LVOT and aortic flows has never been verified and the few CMR studies which showed both LVOT and aortic velocity profiles highlighted obvious differences in waveforms in both early and late systole[44]. CMR, with its velocity-encoded sequences, is already considered to be the reference for LV volumes including stroke volume, myocardial mass and thus global systolic function evaluation. In addition, it has been recently used to estimate aortic stiffness indices[4, 30-33], providing direct

measurements of local aortic elasticity, as well as time-varying aortic blood flow. Therefore, we hypothesized that carotid pressure tonometry data combined with such aortic PC-CMR flow data would enable an accurate estimation of Zc_{Ao}, providing supplementary data on LV load especially regarding the contribution to its pulsatile component.

To our knowledge, this is the first study to report the temporal estimation of Zc_{Ao} using aortic PC-CMR and carotid tonometry data. Another original feature of our study is that seven previously presented methods of characteristic impedance estimation in the time domain[5, 12, 20, 41] that could be easily integrated to a clinical workflow were tested on a group of 93 subjects including healthy volunteers and asymptomatic patients with hypertension. Such methods were based either on peak flow[12], 95% of peak flow[20], pressure at the inflection point[5], stroke volume[41], pressure and flow time derivatives peaks[12], systolic up-slopes[12] or early systolic slope of the pressure-flow loop[12]. For all methods, the resulting values were within the physiological range for both the healthy and hypertensive populations. Indeed, when comparing to studies including healthy subjects with a similar age range, Ting et al.[18] reported a mean value of 112 dyne.s/cm^5 in 8 healthy subjects (mean age: 42 ± 8 years) and Merillon et al.[45] reported a mean value of 101 ± 21 dyne.s/cm^5 in 28 healthy subjects (mean age: 42 ± 15 years), both using invasive techniques. Comparison against larger population studies[21, 28] is rendered difficult by differences in aortic blood flow measurement devices and sites, since in most of them aortic flow was measured in the LVOT using Doppler echocardiography.

We observed no differences in aortic characteristic impedance between young and elderly healthy subjects, regardless of the method. This finding is not inconsistent with literature since discrepancies have been previously reported regarding age-related variation of such index. Indeed, while its increase with age has been demonstrated in 45 healthy subjects[16], a population-based study including 2026 healthy subjects[21] found steady impedance values with age in women and a decrease in men. These differences could be explained by the methods used for impedance calculation: characteristic impedance based on aortic velocity could be excessively increased, since systolic peak velocity decreases with aging as the aorta dilates, resulting in unchanged aortic flow with age. Also, when considering the theoretical water hammer model relating aortic characteristic impedance to aortic pulse wave velocity (PWV) and area ($Zc_{Ao} = \rho \cdot PWV / area$, where ρ is blood density)[45], we can hypothesize that Zc_{Ao} might not increase in elderly subjects due to the parallel age-related increase of both aortic PWV and area. Thus, the age-related dilation of the proximal aorta might express a remodeling process to normalize pulsatile load when aorta stiffens[46]. Finally, the previously described differences in aortic characteristic impedance between men and women, which are more pronounced in elderly subjects [21], were found in our population, demonstrating the reliability of our measurements.

To compare and further assess the reliability of the 7 time domain methods, we tested the ability of characteristic impedance to separate between patients with hypertension and controls. First, values obtained in our hypertensive subjects were close albeit slightly lower than characteristic impedance previously averaged on untreated hypertensive patients (166 dyne.s/cm^5)[18] using catheterization, despite higher blood

pressures in this latter study (mean aortic systolic/diastolic pressures: 168/99 mmHg). In addition, similar to previous literature[18], we found that characteristic impedance was significantly increased in patients with hypertension when compared to the elderly healthy volunteers with a similar age, for the reference frequency method and temporal methods based on 95% of peak flow as well as up-slopes and time derivatives peaks ratios.

Moreover, all time domain methods were significantly correlated to central pulse pressure indicating the pulsatile feature of characteristic impedance and to the reference frequency domain characteristic impedance. Despite these good correlations, time domain methods underestimated characteristic impedance when compared to the frequency domain method. While these underestimations were in line with results of a previous study[47], they differ from those of Segers et al.[21]. Such slight discrepancies between studies could be explained by differences in methods used for impedance estimation. Indeed several frequency ranges for characteristic impedance estimation were proposed in the literature[7, 9, 10, 12, 13, 19, 21]. Furthermore, differences between time and frequency domain impedance estimates might be due to the fact that time domain methods rely only on early systolic up-slopes, while the frequency domain method takes into account the entire cardiac cycle. Furthermore, associations between frequency domain impedance and time domain methods based on 95% of peak flow, derivative peaks and systolic up-slopes were slightly inferior to those previously reported (r=0.96 for the derivative peaks method and r=0.94 for the up-slopes method) in the invasive study presented by Lucas et al.[12]. Such slight difference might be explained by the fact that authors in this latter study studied characteristic impedance in 134 patients from 1 month to 64

years (mean age: 13.5 years) with a congenital septal defect before and/or after closure of the septal defect (262 datasets), resulting in a wide range of characteristic impedance values (approximately between 20 and 1600 dyne.s/cm^5). Correlations obtained for the three aforementioned time domain impedance methods were equivalent to the association reported by Segers et al. on 2026 healthy subjects (mean age: 46 years) (r = 0.82)[21]. The equivalence of the associations of the presented time domain methods with the reference method when comparing against studies on large populations and/or on a large range of characteristic impedance suggests the accuracy of our PC-CMR based impedance measurements that were performed on a relatively small population (frequency domain characteristic impedance ranged between 40 and 310 dyne.s/cm^5).

In addition to their slight superiority in terms of discrimination between hypertensive patients and controls with a similar mean age, and of correlations against carotid pulse pressure or frequency domain reference values, methods based on up-slopes and time derivatives peaks have the advantages of being performed on raw pressure and flow curves, before temporal shift and resizing of the curves, minimizing potential errors created by the fact that central blood pressure and flow were not measured at the same site.

Indeed, a first limitation of our study is that pressure and flow were measured at different arterial sites and not simultaneously, which is required for an accurate estimation of characteristic impedance. However, such simultaneous measurements in the aorta can be performed only using invasive techniques, which cannot be acquired in healthy volunteers. To minimize such errors, pressure was measured using applanation tonometry at the carotid artery which is considered as a good surrogate

for central blood pressure[48] and has been widely used to derive relevant parameters that are strongly associated with cardiovascular events[3]. Moreover, brachial blood pressure measurements acquired simultaneously to PC-CMR aortic imaging were used to calibrate the carotid pressure waveform, based on the assumption that diastolic and mean pressures remain constant between central and peripheral arteries[9, 49]. Another limitation inherent to PC-CMR acquisitions is errors in velocity and flow measurements related to phase-offset. Such errors were minimized using a 50% rectangular field of view centered on the aorta but can be alternatively corrected using techniques presented in previous studies[50]. In addition, our study focused on comparison of various techniques all based on the same data, reducing the effect of such phase-offset errors.

Conclusion

Aortic characteristic impedance estimated in the time domain using PC-CMR and applanation tonometry data along with the straightforward and fast computation derivatives peaks, up-slopes and 95% of peak flow methods that can be easily integrated to a clinical workflow, was able to distinguish patients with hypertension from controls with a similar age and was in good agreement with carotid pulse pressure and with the frequency domain characteristic impedance reference. Such parameter of the pulsatile load facing the LV during its ejection might be complementary to the emerging CMR aortic stiffness and geometry indices[4] to characterize LV-aortic coupling, especially in disease such as arterial hypertension.

Acknowledgment

Ioannis Bargiotas was co-funded through Greek State Scholarship Foundation (IKY) – academic year 2011-2012, by the funds of European Social Fund (ESF) and NSRF, 2007-2013.

References

[1] Laurent S, Cockcroft J, Van Bortel L, Boutouyrie P, Giannattasio C, Hayoz D, et al. Expert consensus document on arterial stiffness: methodological issues and clinical applications. Eur Heart J 2006; 27:2588-2605.

[2] Mitchell GF, Hwang SJ, Vasan RS, Larson MG, Pencina MJ, Hamburg NM, et al. Arterial stiffness and cardiovascular events: the Framingham Heart Study. Circulation 2010; 121:505-511.

[3] Vlachopoulos C, Aznaouridis K, Stefanadis C. Prediction of cardiovascular events and all-cause mortality with arterial stiffness: a systematic review and meta-analysis. J Am Coll Cardiol 2010; 55:1318-1327.

[4] Redheuil A, Yu WC, Mousseaux E, Harouni AA, Kachenoura N, Wu CO, et al. Age-related changes in aortic arch geometry: relationship with proximal aortic function and left ventricular mass and remodeling. J Am Coll Cardiol 2011; 58:1262-1270.

[5] Nichols WW, O'Rourke MF, Vlachopoulos C. McDonald's Blood Flow in Arteries. Theoretical, Experimental and Clinical Principles (6th ed.). London:Edward Arnold 2011:210-212.

[6] Chirinos JA, Segers P, Raina A, Saif H, Swillens A, Gupta AK, et al. Arterial pulsatile hemodynamic load induced by isometric exercise strongly predicts left ventricular mass in hypertension. Am J Physiol Heart Circ Physiol 2009; 298:H320-330.

[7] Binkley PF, Van Fossen DB, Nunziata E, Unverferth DV, Leier CV. Influence of positive inotropic therapy on pulsatile hydraulic load and ventricular-vascular coupling in congestive heart failure. J Am Coll Cardiol 1990; 15:1127-1135.

[8] Gundel W, Cherry G, Rajagopalan B, Tan LB, Lee G, Schultz D. Aortic input impedance in man: acute response to vasodilator drugs. Circulation 1981; 63:1305-1314.

[9] Kelly R, Fitchett D. Noninvasive determination of aortic input impedance and external left ventricular power output: a validation and repeatability study of a new technique. J Am Coll Cardiol 1992; 20:952-963.

[10] Kromer EP, Elsner D, Holmer SR, Muntze A, Riegger GA. Aortic input impedence and neurohormonal activation in patients with mild to moderate chronic congestive heart failure. Cardiovasc Res 1992; 26:265-272.

[11] Laskey WK, Kussmaul WG, Martin JL, Kleaveland JP, Hirshfeld JW, Jr., Shroff S. Characteristics of vascular hydraulic load in patients with heart failure. Circulation 1985; 72:61-71.

[12] Lucas CL, Wilcox BR, Ha B, Henry GW. Comparison of time domain algorithms for estimating aortic characteristic impedance in humans. IEEE Trans Biomed Eng 1988; 35:62-68.

[13] Merillon JP, Fontenier G, Lerallut JF, Jaffrin MY, Chastre J, Assayag P, et al. Aortic input impedance in heart failure: comparison with normal subjects and its changes during vasodilator therapy. Eur Heart J 1984; 5:447-455.

[14] Murgo JP, Westerhof N, Giolma JP, Altobelli SA. Aortic input impedance in normal man: relationship to pressure wave forms. Circulation 1980; 62:105-116.

[15] Nichols WW, Conti CR, Walker WE, Milnor WR. Input impedance of the systemic circulation in man. Circ Res 1977; 40:451-458.

[16] Nichols WW, O'Rourke MF, Avolio AP, Yaginuma T, Murgo JP, Pepine CJ, Conti CR. Effects of age on ventricular-vascular coupling. Am J Cardiol 1985; 55:1179-1184.

[17] Pepine CJ, Nichols WW, Conti CR. Aortic input impedance in heart failure. Circulation 1978; 58:460-465.

[18] Ting CT, Brin KP, Lin SJ, Wang SP, Chang MS, Chiang BN, Yin FC. Arterial hemodynamics in human hypertension. J Clin Invest 1986; 78:1462-1471.

[19] Cholley BP, Shroff SG, Sandelski J, Korcarz C, Balasia BA, Jain S, et al. Differential effects of chronic oral antihypertensive therapies on systemic arterial circulation and ventricular energetics in African-American patients. Circulation 1995; 91:1052-1062.

[20] Mitchell GF, Tardif JC, Arnold JM, Marchiori G, O'Brien TX, Dunlap ME, Pfeffer MA. Pulsatile hemodynamics in congestive heart failure. Hypertension 2001; 38:1433-1439.

[21] Segers P, Rietzschel ER, De Buyzere ML, Vermeersch SJ, De Bacquer D, Van Bortel LM, et al. Noninvasive (input) impedance, pulse wave velocity, and wave reflection in healthy middle-aged men and women. Hypertension 2007; 49:1248-1255.

[22] Dujardin JP, Stone DN. Characteristic impedance of the proximal aorta determined in the time and frequency domain: a comparison. Med Biol Eng Comput 1981; 19:565-568.

[23] Levy BI, Babalis D, Lacolley P, Poitevin P, Safar ME. Cardiac hypertrophy and characteristic impedance in spontaneously hypertensive rats. J Hypertens Suppl 1988; 6:S110-111.

[24] Li JK. Time domain resolution of forward and reflected waves in the aorta. IEEE Trans Biomed Eng 1986; 33:783-785.

[25] Mitchell GF, Gudnason V, Launer LJ, Aspelund T, Harris TB. Hemodynamics of increased pulse pressure in older women in the community-based Age, Gene/Environment Susceptibility-Reykjavik Study. Hypertension 2008; 51:1123-1128.

[26] Mitchell GF, Izzo JL, Jr., Lacourciere Y, Ouellet JP, Neutel J, Qian C, et al. Omapatrilat reduces pulse pressure and proximal aortic stiffness in patients with systolic hypertension: results of the conduit hemodynamics of omapatrilat international research study. Circulation 2002; 105:2955-2961.

[27] Mitchell GF, Lacourciere Y, Ouellet JP, Izzo JL, Jr., Neutel J, Kerwin LJ, et al. Determinants of elevated pulse pressure in middle-aged and older subjects with uncomplicated systolic hypertension: the role of proximal aortic diameter and the aortic pressure-flow relationship. Circulation 2003; 108:1592-1598.

[28] Mitchell GF, van Buchem MA, Sigurdsson S, Gotal JD, Jonsdottir MK, Kjartansson O, et al. Arterial stiffness, pressure and flow pulsatility and brain structure and function: the Age, Gene/Environment Susceptibility--Reykjavik study. Brain 2011; 134:3398-3407.

[29] Sweitzer NK, Shenoy M, Stein JH, Keles S, Palta M, LeCaire T, Mitchell GF. Increases in central aortic impedance precede alterations in arterial stiffness measures in type 1 diabetes. Diabetes Care 2007; 30:2886-2891.

[30] Dogui A, Kachenoura N, Frouin F, Lefort M, De Cesare A, Mousseaux E, Herment A. Consistency of aortic distensibility and pulse wave velocity estimates with respect to the Bramwell-Hill theoretical model: a cardiovascular magnetic resonance study. J Cardiovasc Magn Reson 2011; 13:11.

[31] Dogui A, Redheuil A, Lefort M, DeCesare A, Kachenoura N, Herment A, Mousseaux E. Measurement of aortic arch pulse wave velocity in cardiovascular MR: comparison of transit time estimators and description of a new approach. J Magn Reson Imaging 2011; 33:1321-1329.

[32] Grotenhuis HB, Ottenkamp J, Westenberg JJ, Bax JJ, Kroft LJ, de Roos A. Reduced aortic elasticity and dilatation are associated with aortic regurgitation and left ventricular hypertrophy in nonstenotic bicuspid aortic valve patients. J Am Coll Cardiol 2007; 49:1660-1665.

[33] Redheuil A, Yu WC, Wu CO, Mousseaux E, de Cesare A, Yan R, et al. Reduced ascending aortic strain and distensibility: earliest manifestations of vascular aging in humans. Hypertension 2010; 55:319-326.

[34] Firmin DN, Nayler GL, Kilner PJ, Longmore DB. The application of phase shifts in NMR for flow measurement. Magn Reson Med 1990; 14:230-241.

[35] Gatehouse PD, Keegan J, Crowe LA, Masood S, Mohiaddin RH, Kreitner KF, Firmin DN. Applications of phase-contrast flow and velocity imaging in cardiovascular MRI. Eur Radiol 2005; 15:2172-2184.

[36] Segers P, De Backer J, Devos D, Rabben SI, Gillebert TC, Van Bortel LM, et al. Aortic reflection coefficients and their association with global indexes of wave reflection in healthy controls and patients with Marfan's syndrome. Am J Physiol Heart Circ Physiol 2006; 290:H2385-2392.

[37] Salvi P, Lio G, Labat C, Ricci E, Pannier B, Benetos A. Validation of a new non-invasive portable tonometer for determining arterial pressure wave and pulse wave velocity: the PulsePen device. J Hypertens 2004; 22:2285-2293.

[38] Herment A, Kachenoura N, Lefort M, Bensalah M, Dogui A, Frouin F, et al. Automated segmentation of the aorta from phase contrast MR images: validation against expert tracing in healthy volunteers and in patients with a dilated aorta. J Magn Reson Imaging 2010; 31:881-888.

[39] Corden B, Keenan NG, de Marvao AS, Dawes TJ, Decesare A, Diamond T, et al. Body fat is associated with reduced aortic stiffness until middle age. Hypertension 2013; 61:1322-1327.

[40] Westenberg JJ, van Poelgeest EP, Steendijk P, Grotenhuis HB, Jukema JW, de Roos A. Bramwell-Hill modeling for local aortic pulse wave velocity estimation: a validation study with velocity-encoded cardiovascular magnetic resonance and invasive pressure assessment. J Cardiovasc Magn Reson 2012; 14:2.

[41] Chemla D, Plamann K, Nitenberg A. Towards new indices of arterial stiffness using systolic pulse contour analysis: a theoretical point of view. J Cardiovasc Pharmacol 2008; 51:111-117.

[42] Mitchell GF, Pfeffer MA, Westerhof N, Pfeffer JM. Measurement of aortic input impedance in rats. Am J Physiol 1994; 267:H1907-1915.

[43] Sheskin DJ. Handbook of Parametric and Nonparametric Statistical Procedures: Third Edition. Chapman and Hall/CRC 2003:973-974.

[44] Garcia J, Kadem L, Larose E, Clavel MA, Pibarot P. Comparison between cardiovascular magnetic resonance and transthoracic Doppler echocardiography for the estimation of effective orifice area in aortic stenosis. J Cardiovasc Magn Reson 2011; 13:25.

[45] Merillon JP, Motte G, Masquet C, Azancot I, Guiomard A, Gourgon R. Relationship between physical properties of the arterial system and left ventricular performance in the course of aging and arterial hypertension. Eur Heart J 1982; 3 Suppl A:95-102.

[46] Mitchell GF, Wang N, Palmisano JN, Larson MG, Hamburg NM, Vita JA, et al. Hemodynamic correlates of blood pressure across the adult age spectrum: noninvasive evaluation in the Framingham Heart Study. Circulation 2010; 122:1379-1386.

[47] Nichols WW, O'Rourke MF, Vlachopoulos C. McDonald's Blood Flow in Arteries. Theoretical, Experimental and Clinical Principles (6th ed.). London:Edward Arnold 2011:91-93.

[48] Van Bortel LM, Balkestein EJ, van der Heijden-Spek JJ, Vanmolkot FH, Staessen JA, Kragten JA, et al. Non-invasive assessment of local arterial pulse pressure: comparison of applanation tonometry and echo-tracking. J Hypertens 2001; 19:1037-1044.

[49] Borow KM, Newburger JW. Noninvasive estimation of central aortic pressure using the oscillometric method for analyzing systemic artery pulsatile blood flow: comparative study of indirect systolic, diastolic, and mean brachial artery pressure with simultaneous direct ascending aortic pressure measurements. Am Heart J 1982; 103:879-886.

[50] Chernobelsky A, Shubayev O, Comeau CR, Wolff SD. Baseline correction of phase contrast images improves quantification of blood flow in the great vessels. J Cardiovasc Magn Reson 2007; 9:681-685.

Tables

Table 1 - Subjects baseline characteristics, central blood pressures, aortic geometry and stiffness indices as well as aortic characteristic impedance estimated in frequency and time domains averaged for healthy young (below 50 years) and elderly (above 50 years) subjects as well as hypertensive patients.

Parameters	Young subjects (n = 45)	Elderly subjects (n = 32)	Hypertensive subjects (n = 16)
Age (years)	32 ± 9	59 ± 8*	61 ± 9
Gender (males/females)	28/17	18/14	11/5
Weight (kg)	69 ± 12	71 ± 10	77 ± 16
Height (cm)	173 ± 8	171 ± 8	170 ± 8
BSA (m^2)	1.82 ± 0.19	1.83 ± 0.16	1.88 ± 0.23
BMI (kg/m^2)	23.0 ± 2.9	24.3 ± 2.7	26.2 ± 3.9†
Heart rate (bpm)	67 ± 11	63 ± 12	64 ± 9
Carotid systolic blood pressure (mmHg)	99 ± 9	109 ± 15*	116 ± 20
Carotid diastolic blood pressure (mmHg)	64 ± 9	74 ± 10*	75 ± 14
Mean blood pressure (mmHg)	82 ± 8	92 ± 11*	95 ± 17
Carotid pulse pressure (mmHg)	34 ± 6	35 ± 12	41 ± 9†
CMR AA diastolic diameter (mm)	25.8 ± 3.0	31.6 ± 3.6*	31.5 ± 0.3
CMR AA pulse wave velocity (m/s)	4.5 ± 0.8	7.5 ± 4.2*	8.8 ± 3.7
Zc_{AoF} ($dyne.s/cm^5$)	120 ± 37	133 ± 67	176 ± 64†
Zc_{AoQmax} ($dyne.s/cm^5$)	119 ± 28	111 ± 40	130 ± 47
$Zc_{AoQ95\%max}$ ($dyne.s/cm^5$)	109 ± 25	104 ± 39	130 ± 45†
Zc_{AoPi} ($dyne.s/cm^5$)	116 ± 28	132 ± 50	142 ± 59
Zc_{AoSV} ($dyne.s/cm^5$)	90 ± 22	106 ± 40	116 ± 54
$Zc_{Aoslopes}$ ($dyne.s/cm^5$)	99 ± 26	103 ± 48	137 ± 58†
$Zc_{Aoderiv}$ ($dyne.s/cm^5$)	116 ± 36	132 ± 61	175 ± 74†
Zc_{Aoloop} ($dyne.s/cm^5$)	105 ± 30	121 ± 64	152 ± 61

Young subjects are < 50 years old; elderly subjects are ≥ 50 years old.

BSA: body surface area; BMI: body mass index; CMR: cardiovascular magnetic resonance; AA: ascending aorta; Zc_{AoF}: aortic characteristic impedance estimated in the frequency domain; Time domain Zc_{AoQmax}: based on peak flow; $Zc_{AoQ95\%max}$: based on 95% of peak flow; Zc_{AoPi}: based on pressure at the inflection point; Zc_{AoSV}: based on stroke volume; $Zc_{Aoslopes}$: based on systolic up-slopes; $Zc_{Aoderiv}$: based on time-derivatives peaks; Zc_{Aoloop}: based on early systolic slope of the pressure-flow loop.

Indices are provided as mean values ± standard deviations.

* indicates a p value < 0.05 for comparison between the elderly and the young subjects groups. † indicates a p value < 0.05 for comparison between the hypertensive and the elderly subjects groups.

Table 2 - Comparisons of time domain aortic characteristic impedance against pulse pressure and the frequency reference values.

	Carotid pulse pressure	Frequency domain Zc_{Ao}	
	r	r	Bland-Altman biases (dyne.s/cm^5)
1) Zc_{AoQmax}	0.50*	0.69*	–9 [-84;65]
2) $Zc_{AoQ95\%max}$	0.49*	0.82*	–18 [-81;44]
3) Zc_{AoPi}	0.50*	0.65*	–3 [-81;75]
4) Zc_{AoSV}	0.44†	0.65*	–29 [-106;49]
5) $Zc_{Aoslopes}$	0.52*	0.86*	–25 [-80;30]
6) $Zc_{Aoderiv}$	0.49*	0.82*	–2 [-62;57]
7) Zc_{Aoloop}	0.33†	0.73*	–14 [-86;59]

Zc_{Ao}: aortic characteristic impedance; Time domain Zc_{AoQmax}: based on peak flow; $Zc_{AoQ95\%max}$: based on 95% of peak flow; Zc_{AoPi}: based on pressure at the inflection point; Zc_{AoSV}: based on stroke volume; $Zc_{Aoslopes}$: based on systolic up-slopes; $Zc_{Aoderiv}$: based on time-derivatives peaks; Zc_{Aoloop}: based on early systolic slope of the pressure-flow loop.

Pearson correlation coefficients and Bland-Altman biases (defined as the averaged temporal value – frequency value) as well as limits of agreement (defined as [mean bias-1.96xSD; mean bias+1.96xSD]) are provided.

* indicates $p<0.0001$ and † indicates $p<0.005$.

Figure captions

Figure 1 – A. Illustration on a sagittal view of the positioning (red line) of CMR axial plane for measurement of mid-ascending aortic areas and through-plane velocities. B. Systolic modulus image of the mid-ascending aorta and C. the corresponding through-plane velocity image. Of note, aortic contours automatically detected on modulus images and then superimposed on velocity images for flow estimation are illustrated in white.

Figure 2 - Semi-automated measurement of time domain (A-C) and frequency domain (D) aortic characteristic impedance from PC-CMR and applanation tonometry data. A. Carotid pressure and aortic flow curves on which specific values were used for methods 1 to 4. Pressure and flow early systolic up-slopes used for method 5 are also illustrated (red lines). B. Carotid pressure and aortic flow time derivatives (method 6). C. Early systolic slope of the pressure-flow loop (method 7, red line). D. Input impedance magnitude, calculated for each harmonic as the ratio between fast Fourier transform moduli of pressure and flow. The interval used for frequency characteristic impedance is illustrated in purple. See text for more details on methods 1 to 7 in the time domain and the reference method in the frequency domain.

Figure 3 - Input impedance spectra averaged over the groups of young healthy subjects (solid line), elderly healthy subjects (dashed line) and elderly hypertensive patients (dotted line), with a special emphasis (purple box) on the interval used for characteristic impedance estimation.

Figure 4 - Aortic characteristic impedance values obtained in our healthy subjects using the frequency method (left) and the temporal method based on 95% of peak flow (right), averaged within each age group for women (white bars) and for men

(black bars). Differences were tested using the nonparametric Mann–Whitney test and * indicates $p<0.05$.

Figures

Figure 1

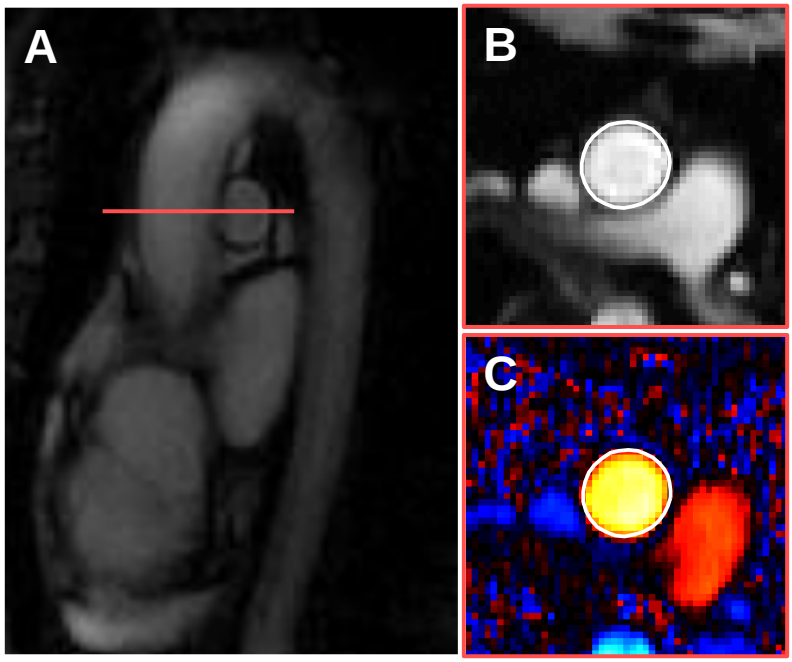

Figure 2

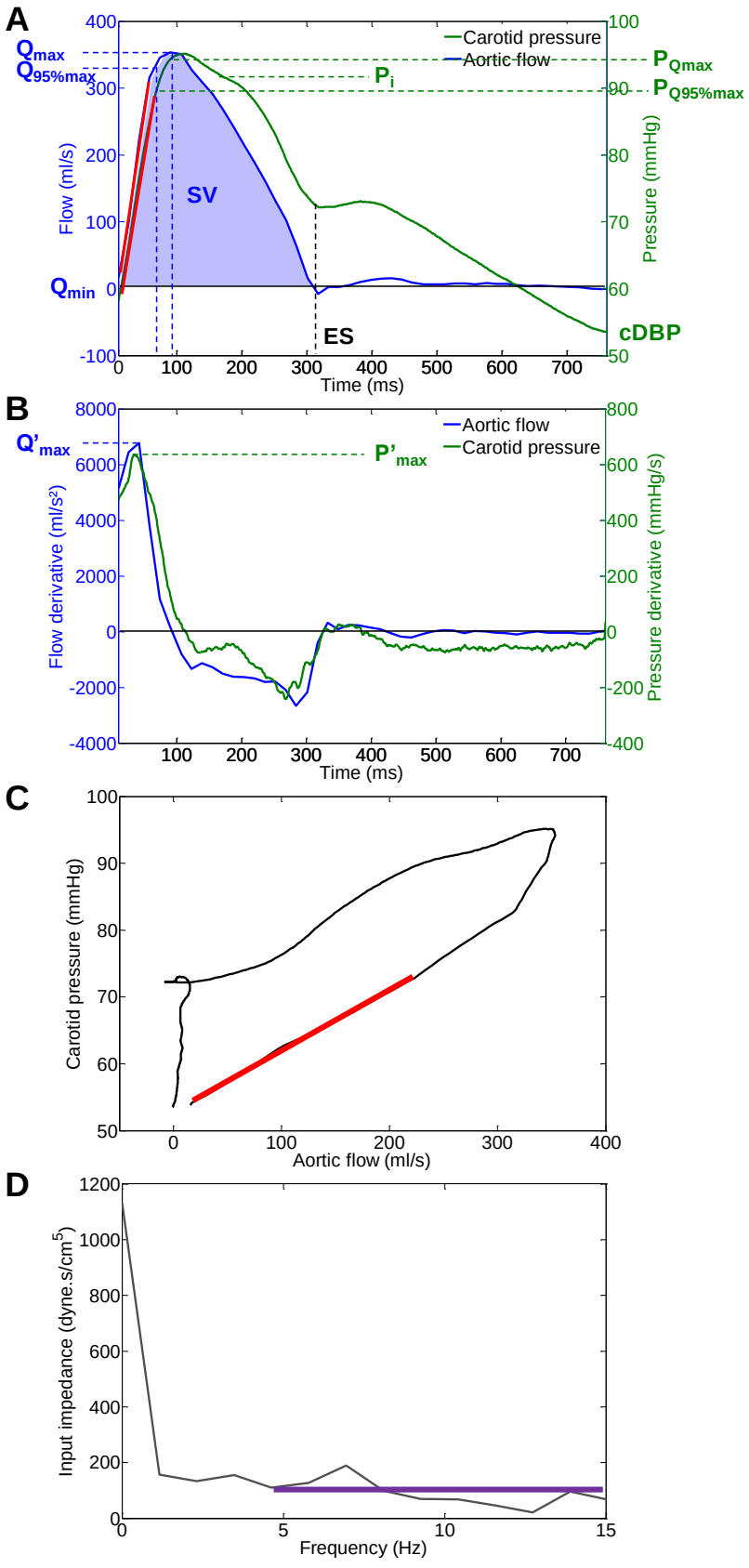
A
Qmax
Q95%max
Pi
PQmax
PQ95%max
Carotid pressure
Aortic flow
SV
Qmin
ES
cDBP
Flow (ml/s)
Pressure (mmHg)
Time (ms)
B
Q'max
P'max
Aortic flow
Carotid pressure
Flow derivative (ml/s²)
Pressure derivative (mmHg/s)
Time (ms)
C
Carotid pressure (mmHg)
Aortic flow (ml/s)
D
Input impedance (dyne.s/cm⁵)
Frequency (Hz)

Figure 3

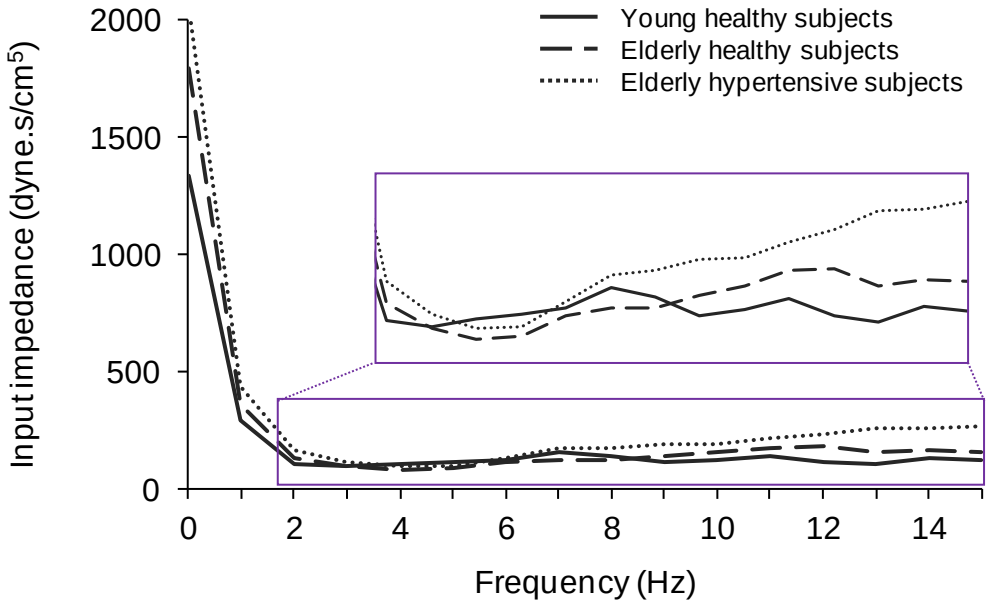
Young healthy subjects
Elderly healthy subjects
Elderly hypertensive subjects
Input impedance (dyne.s/cm5)
2000
1500
1000
500
0
0
2
4
6
8
10
12
14
Frequency (Hz)

Figure 4

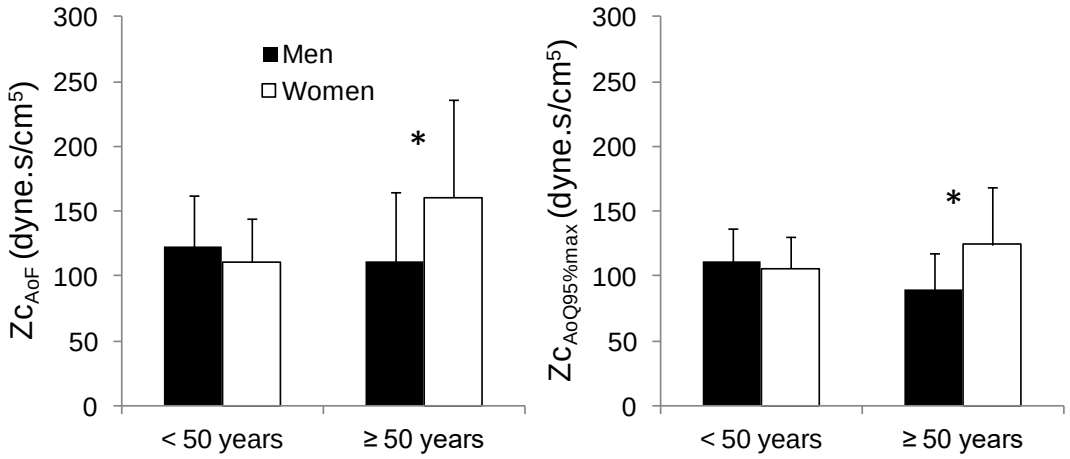
300
250
200
150
100
50
0
Men
Women
Zc_{AoF} (dyne.s/cm^5)
*
< 50 years
≥ 50 years
$Zc_{AoQ95\%max}$ (dyne.s/cm^5)
*
< 50 years
≥ 50 years